ISSN 0006-2979, Biochemistry (Moscow), 2009, Vol. 74, No. 7, pp. 756-765. © Pleiades Publishing, Ltd., 2009.
Original Russian Text © Z. O. Shenkarev, E. N. Lyukmanova, O. I. Solozhenkin, I. E. Gagnidze, O. V. Nekrasova, V. V. Chupin, A. A. Tagaev, Z. A. Yakimenko, T. V. Ovchinnikova, M. P. Kirpichnikov, A. S. Arseniev, 2009, published in Biokhimiya, 2009, Vol. 74, No. 7, pp. 933-945.
Originally published in Biochemistry (Moscow) On-Line Papers in Press, as Manuscript BM09-026, May 10, 2009.

Lipid–Protein Nanodiscs: Possible Application in High-Resolution NMR Investigations of Membrane Proteins and Membrane-Active Peptides

Z. O. Shenkarev*, E. N. Lyukmanova, O. I. Solozhenkin, I. E. Gagnidze, O. V. Nekrasova, V. V. Chupin, A. A. Tagaev, Z. A. Yakimenko, T. V. Ovchinnikova, M. P. Kirpichnikov, and A. S. Arseniev*

Shemyakin–Ovchinnikov Institute of Bioorganic Chemistry, Russian Academy of Sciences, ul. Miklukho-Maklaya 16/10, 117997 Moscow, Russia; fax: (495) 335-5033; E-mail: zh@nmr.ru; aars@nmr.ru

Received January 26, 2009
Revision received February 6, 2009

Abstract—High-resolution NMR is shown to be applicable for investigation of membrane proteins and membrane-active peptides embedded into lipid–protein nanodiscs (LPNs). ^{15}N-Labeled K^+-channel from *Streptomyces lividans* (KcsA) and the antibiotic antiamoebin I from *Emericellopsis minima* (Aam-I) were embedded in LPNs of different lipid composition. Formation of stable complexes undergoing isotropic motion in solution was confirmed by size-exclusion chromatography and ^{31}P-NMR spectroscopy. The 2D ^{1}H-^{15}N-correlation spectra were recorded for KcsA in the complex with LPN containing DMPC and for Aam-I in LPNs based on DOPG, DLPC, DMPC, and POPC. The spectra recorded were compared with those in detergent-containing micelles and small bicelles commonly used in high-resolution NMR spectroscopy of membrane proteins. The spectra recorded in LPN environments demonstrated similar signal dispersion but significantly increased ^1H_N line width. The spectra of Aam-I embedded in LPNs containing phosphatidylcholine showed significant selective line broadening, thus suggesting exchange process(es) between several membrane-bound states of the peptide. ^{15}N relaxation rates were measured to obtain the effective rotational correlation time of the Aam-I molecule. The obtained value (~40 nsec at 45°C) is indicative of additional peptide motions within the Aam-I/LPN complex.

DOI: 10.1134/S0006297909070086

Key words: nanodisc, apolipoprotein, high-density lipoprotein particle, membrane protein, membrane-active peptide, model membranes, NMR spectroscopy

High-resolution NMR-spectroscopy is a widely used method for investigation of protein molecular structures in solutions [1, 2]. Novel experimental methods and advanced approaches to preparation of isotope-labeled protein molecules have significantly extended the applicability of NMR-spectroscopy to studies of large proteins and supramolecular complexes. Uniform side chain deuteration [3] and special relaxation optimized NMR experiments (TROSY, CRINEPT) can now be used for determination of spatial structures of proteins with

Abbreviations: Aam-I, antibiotic antiamoebin I from *Emericellopsis minima*; apoA-1, apolipoprotein A-1; CRINEPT, cross-correlated relaxation-enhanced polarization; 1D, one-dimensional; 2D, two-dimensional; DDM, β-dodecyl maltoside; DHPC, dihexanoyl phosphatidylcholine; DLPC, dilauroyl phosphatidylcholine; DLPG, dilauroyl phosphatidylglycerol; DMPC, dimyristoyl phosphatidylcholine; DOPC, dioleoyl phosphatidylcholine; DOPE, dioleoyl phosphatidylethanolamine; DOPG, dioleoyl phosphatidylglycerol; HMQC, heteronuclear multiple quantum correlation; HSQC, heteronuclear single quantum correlation; INEPT, insensitive nuclei enhanced by polarization transfer; KcsA, K^+-channel from *Streptomyces lividans*; LMPC, lysomyristoyl phosphatidylcholine; LMPG, lysomyristoyl phosphatidylglycerol; LPN, lipid–protein nanodisc; MP, membrane protein; MSP, fragment 44-243 of human apolipoprotein A1 (membrane scaffold protein); POPC, palmitoyloleoyl phosphatidylcholine; R_{St}, hydrodynamic radius of a particle, Stokes radius; TM, transmembrane; TROSY, transverse relaxation-optimized spectroscopy; $\Delta\nu$, half-peak width of NMR band; η_{XY}, rate of cross-correlation between dipole–dipole and chemical shift anisotropy relaxation of the ^{15}N nucleus; τ_R, effective rotational correlation time.

* To whom correspondence should be addressed.

molecular masses up to 100 kDa and examination of protein–protein complexes with molecular masses up to 1000 kDa [4-7]. Unfortunately, the progress achieved is mainly for water-soluble proteins and it does not facilitate studies of another important class of protein molecules – membrane proteins (MP) [8].

The main difficulty in NMR studies of MP is the search for a suitable solubilizing medium (membrane mimetic) [8-10]. An ideal membrane mimetic has to support the native (functional) protein structure and, at the same time provide "interpretable" NMR spectra of the solubilized molecule. At the initial stages of analysis, the spectrum quality is estimated in terms of signal dispersion and spectral line width. However, the width of NMR signals significantly increases with increase in size of a complex (protein/membrane mimetic under study). As a result, membrane-mimicking media based on real bilayer membranes in the form of vesicles or large bicelles cannot be used in high-resolution NMR spectroscopy.

Membrane mimetics commonly used in NMR studies have some drawbacks. In particular, organic solvents with low polarity, such as methanol, trifluoroethanol, or methanol/chloroform and trifluoroethanol/water mixtures, are isotropic in their nature and have little applicability as models of biological membrane [8]. On the other hand, anisotropic membrane mimetics (detergent micelles and small spherical lipid/detergent bicelles) have significant surface curvature [8-10], which can seriously distort the spatial structure of the solubilized protein [11]. Moreover, high lability of detergent-containing complexes often increases intramolecular mobility of α-helical MPs, which can lead to significant broadening and weakening of NMR signals from transmembrane domains (TMs) [8-10]. Instability of micellar complexes below the critical micelle concentration also hampers manipulations with samples, such as variations of protein concentration or buffer composition.

In our search for an alternative medium for NMR studies of MPs, we concentrated our attention on reconstructed nascent high-density lipoprotein particles (lipid–protein nanodiscs, LPN). These particles are composed of a bilayer membrane fragment (~160 lipid molecules) surrounded by an apolipoprotein A-1 (apoA-1) dimer. According to the newest models [12-14], LPNs are discs ~10-12 nm in diameter and ~4 nm in thickness (Scheme) coinciding with that of biological membrane. LPN reconstruction *in vitro* was first described more than 20 years ago [15] and was recently adapted for MP solu-

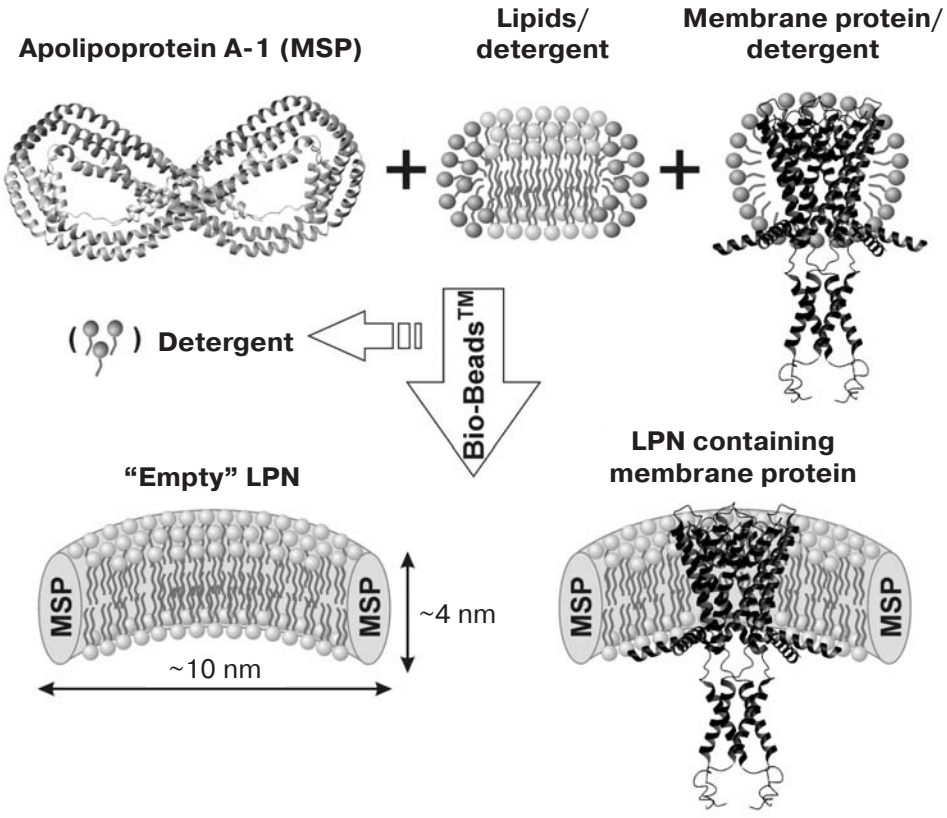

Scheme of reconstruction of MP/LPN complex based on the example of KcsA. Molecules of MSP and KcsA are shown in band representation based on 1AV1 and 1F6G structures (www.pdb.org). Lipid molecules are drawn in light gray and detergent molecules in dark gray. Two MSP molecules shielding the membrane fragment of the nanodisc from solvent are drawn as tori

bilization [16-19]. The lipid membrane fragment of LPN retains many biophysical properties of natural bilayer systems, in particular, an expressed phase transition of lipids from gel to liquid-crystal state is observed in nanodiscs [20]. LPNs possess excellent membrane-mimicking properties and elevated stability compared with traditional membrane mimetics and are thus attractive media for NMR studies of MPs.

The present work is devoted to elaboration of novel approaches to structural studies of membrane proteins and peptides by NMR-spectroscopy using nanodiscs.

MATERIALS AND METHODS

Expression of the *MSP* gene. The *MSP* gene encoding fragment 44-243 of human apoA-1 and carrying an additional N-terminal sequence encoding six His residues and a site for specific hydrolysis by protease TEV was constructed from 18 synthetic overlapped oligonucleotides on the basis of the reported sequence [21, 22] using three-stage PCR. The constructed gene was cloned in the expression vector *pET-28a*(+) (Novagen, USA) at the *Nco*I and *Hin*dIII restriction sites [23]. Bacterial production of MSP in strain BL21(DE3) was carried out on rich medium according to previously developed protocols [21, 22].

Isolation and purification of MSP. Cell culture was centrifuged for 30 min at 2500 rpm and 4°C. The cell pellet from 1 liter of culture was resuspended in 40 ml of buffer A (20 mM Tris-HCl, pH 8.0, 0.5 M NaCl, and 1 mM NaN_3) containing 1% Triton X-100. The cells were disrupted using an ultrasonic disintegrator (Badelin Electronic GmbH, UK) for 10 sec with 10 repeats. Lysate was centrifuged for 30 min at 30,000*g*, and the supernatant was collected. The protein was purified on a Ni^{2+}-Sepharose 6 Fast Flow metal-affinity resin column (GE Healthcare, USA) equilibrated with buffer A containing 1% Triton X-100. Following the sample application, the column was sequentially washed with buffer A containing 1% Triton X-100, buffer A containing 50 mM of sodium cholate, buffer A, and buffer A containing 50 mM of imidazole, four volumes each. MSP was eluted with the buffer A containing 0.5 M of imidazole. The purified MSP was dialyzed against 10 mM Tris-HCl, pH 7.4, containing 100 mM NaCl and 1 mM NaN_3. Protein concentration was determined from absorption at 280 nm using the corresponding molar extinction coefficient. The yield of final product was 150-200 mg/liter of bacterial culture.

Reconstruction and purification of "empty" lipid–protein nanodiscs. Purified MSP was mixed with lipids in molar ratio 1 : 75 in the presence of sodium cholate (the molar ratio cholate/lipids was 2 : 1) and incubated for 3 h at 4°C. When saturated lipids (DMPC, DLPC) were used, the reaction temperature was maintained at no less than 25°C. Self-assembly of nanodiscs was initiated by sorption of the detergent on the Bio-Beads™ resin (Bio-Rad, USA) for 1.5 h. The supernatant contained a mixture of LPN, free MSP, and lipid vesicles. Nanodiscs were purified on metal-affinity resin equilibrated with the buffer A. Following application of reaction mixture, the resin was washed with four volumes of buffer A. LPNs were eluted with buffer A containing 100 mM imidazole.

Reconstruction of lipid–protein nanodiscs containing KcsA. A recombinant gene encoding K^+-channel from *Streptomyces lividans* (KcsA) (homotetramer of 18.3-kDa subunits) was cloned and expressed as described earlier [24]. ^{15}N-Labeled KcsA was produced on minimal medium M9 containing $^{15}NH_4Cl$ as a nitrogen source (Cambridge Isotope Laboratory, USA). KcsA was isolated from biomass according to the method published in [25]. The BL21(DE3) cells containing KcsA were disrupted by sonication, and the cell lysate was centrifuged at 80,000*g* for 1 h. The pellet was solubilized in 0.1 M Na-phosphate buffer, pH 7.0, containing 5 mM of KCl and 15 mM of β-dodecyl maltoside (DDM). The target protein was purified on metal affinity resin. The purified KcsA in 50 mM Tris-HCl buffer, pH 7.5, containing 10 mM KCl and 10 mM DDM was used for LPN preparation. The KcsA sample was mixed with MSP, lipids, and sodium cholate at 1 : 20 : 800 : 1600 molar ratio. The final KcsA concentration was 26 μM. The mixture was incubated overnight with moderate shaking at 4°C for unsaturated lipids (DOPC, POPC) and 25°C for saturated lipids (DMPC). Then Bio-Beads™ resin was added to the mixture followed by additional incubation under vigorous shaking for 2 h at 4 or 25°C depending on the lipids used. The final mixture of liposomes, empty LPN, or LPN containing KcsA was fractionated using metal affinity resin preliminary equilibrated with buffer A. The fraction of nanodiscs containing KcsA was eluted with buffer A containing 500 mM imidazole, dialyzed against 20 mM Tris-HCl, pH 6.9, containing 5 mM KCl, 1 mM EDTA, and 1 mM NaN_3, and concentrated using an ultrafiltration cell NMWL 10000 (Millipore, USA). Protein concentration was determined by absorbance at 280 nm.

Incorporation of antiamoebin in nanodiscs, micelles, and bicelles. ^{15}N-Labeled 1.7-kDa Aam-I (antibiotic antiamoebin I from *Emericellopsis minima*) was prepared as described earlier [26]. The peptide solution in deuterated methanol (C^2H_3OH) at the concentration of 15 mg/ml was prepared for the incorporation of antiamoebin in nanodiscs. The 0.1 mM nanodisc solution in buffer containing 10 mM Tris-acetate, pH 7.0, 1 mM EDTA, and 5% D_2O (total volume 500 μl) was titrated with 4-μl aliquots of antiamoebin followed by incubation in Eppendorf (USA) tubes with open lids under moderate agitation for 1 h at 30°C. The procedure was repeated seven times for preparation of samples for NMR spectrum recording. The final peptide concentration was ~0.5 mM (~5 peptide molecules per disc). The final

methanol concentration in the sample did not exceed 2% according to the ^{2}H-NMR data.

To prepare Aam-I complexes with micelles and bicelles, the preliminarily prepared solutions of detergents and lipids were added to dry weighed samples of the peptide. In all cases, the peptide/detergent molar ratio was no less than 1 : 200. Three sequential freeze–thaw cycles were used for bicelle formation (DMPC/DHPC ratio was 1 : 4).

Size-exclusion chromatography. Size-exclusion chromatography was carried out on a Tricorn 5/200 column (GE Healthcare, Sweden) with Superdex 200 equilibrated with buffer containing 10 mM Tris-HCl, pH 7.4, 100 mM NaCl, 1 mM EDTA, and 1 mM NaN_3. Thyroglobulin (669 kDa, Stokes radius R_{St} = 8.5 nm), ferritin (440 kDa, R_{St} = 6.1 nm), catalase (232 kDa, R_{St} = 5.22 nm), aldolase (158 kDa, R_{St} = 4.81 nm), BSA (67 kDa, R_{St} = 3.55 nm), and ovalbumin (43 kDa, R_{St} = 3.05 nm) were used as standards. The flow rate was 0.3 ml/min, and the protein fractions were detected spectrophotometrically at 280 nm. Particle size was determined from the calibration plot of elution volume against logR_{St}. Considering non-spherical shape of LPN, we supposed that observed R_{St} values correspond to half-diameter of the disc. All particle size (diameter) values below correspond to the doubled R_{St} values.

NMR spectroscopy. 1D ^{1}H-, 1D ^{2}H-, and 2D ^{1}H-^{15}N NMR spectra were recorded at 40-45°C on AVANCE-700 and AVANCE-III-800 spectrometers (Bruker, Germany) equipped with cryogenically-cooled triple-resonance probes with ^{1}H working frequencies 700 and 800 MHz, respectively. The 1D ^{31}P-NMR spectra were recorded at 25°C on an ECA-600 spectrometer (JEOL, Japan) with ^{1}H working frequency of 600 MHz. Chemical shifts of protons were measured relative to residual signal from protons of water, whose chemical shift is 4.75 ppm at 30°C. Chemical shifts of ^{15}N nuclei were calculated using the corresponding gyromagnetic ratio [27]. Chemical shifts of ^{31}P nuclei were measured relative to the signal of the phosphate moiety of DMPC dissolved in sodium cholate, whose chemical shift is –0.5 ppm at 25°C [28].

The rate of cross-correlation between dipole–dipole relaxation and relaxation due to anisotropy of chemical shift of ^{15}N nuclei (η_{XY}) of Aam-I in complex with LPN/DLPC was measured at 45°C on the AVANCE-III-800 spectrometer using the 1D TRACT method [29]. Effective rotational correlation time (τ_R) of the peptide in the complex was calculated from the measured η_{XY} value using known equations [29].

RESULTS

Theoretical background for application of nanodiscs as membrane mimetics in NMR structural studies. Theoretical calculations of rotational diffusion tensor of a discoid particle 10 × 4 nm in size (Scheme) were performed using published analytical equations [30]. The rotational correlation times τA, τB, and τC at 45°C are 56, 57, and 61 nsec, respectively, which corresponds to isotropic rotation of globular protein with hydrodynamic radius R_{St} ~ 4.7 nm and molecular mass ranging within 150-200 kDa. A complex composed of membrane protein and nanodisc seems to exhibit similar dynamic and relaxation properties and, hence, comparable line width in NMR spectra, ^1H_N Δν ~ 90-100 Hz. Comparison of these estimations with data of recent NMR studies of globular proteins (see introductory part) points to a theoretical possibility of measurement of NMR spectra for MP/LPN complexes using TROSY and modern high-field (800-900 MHz) NMR spectrometers.

Practical aspects of protein/LPN complex preparation for NMR spectroscopy. Previously reported methods for reconstruction of nascent high-density lipoprotein particles or lipid–protein nanodiscs *in vitro* are based on addition of detergent solution of lipids to MSP followed by gradual removal of detergent by dialysis [12, 15, 21, 22], gel filtration [19], or application of a special sorbent Bio-Beads™ [16-18]. On removal of detergent from the reaction mixture, self-assembly of nanodiscs occurs (Scheme). To incorporate MP into LPNs, the micellar solution of the target protein should be added to the reaction mixture together with MSP, lipids, and detergents. After removal of detergent, the sample represents a heterogeneous mixture of lipid vesicles, free MSP (soluble aggregates of various stoichiometry), "empty" nanodiscs, and nanodiscs containing MP. It should be noted, that relative population of these components depends on initial composition of the reaction mixture. In particular, contents of both vesicles and free MSP can be decreased by lowering the initial concentrations of lipids and MSP. However, low contents of lipids and MSP during nanodisc formation can result in either irreversible precipitation of the target MP or embedding of several MP molecules in the membrane of one nanodisc. On the other hand, high levels of lipids and MSP in the reaction mixture decreases efficacy of MP embedding in the nanodisc membrane, thus facilitating the formation of side complexes MP/lipid vesicle and MP/MSP.

Since a heterogeneous mixture of components is formed during nanodisc formation, additional steps of chromatographic purification are necessary. Our data show that gel filtration cannot separate LPN from free MSP aggregates of similar size (~10.1 nm) (Fig. 1a and the table), so in our study we used an MSP sequence carrying six histidine residues at the N-terminus of the molecule. This allowed fractionation of lipid vesicles (elution with buffer A), "empty" LPN (elution with 100 mM imidazole), and MSP aggregates (elution with 500 mM imidazole) using Ni^{2+} affinity chromatography. It is worth noting that incorporation of additional sequences, such as FLAG, STREP, or His6 (with pre-elimination of histi-

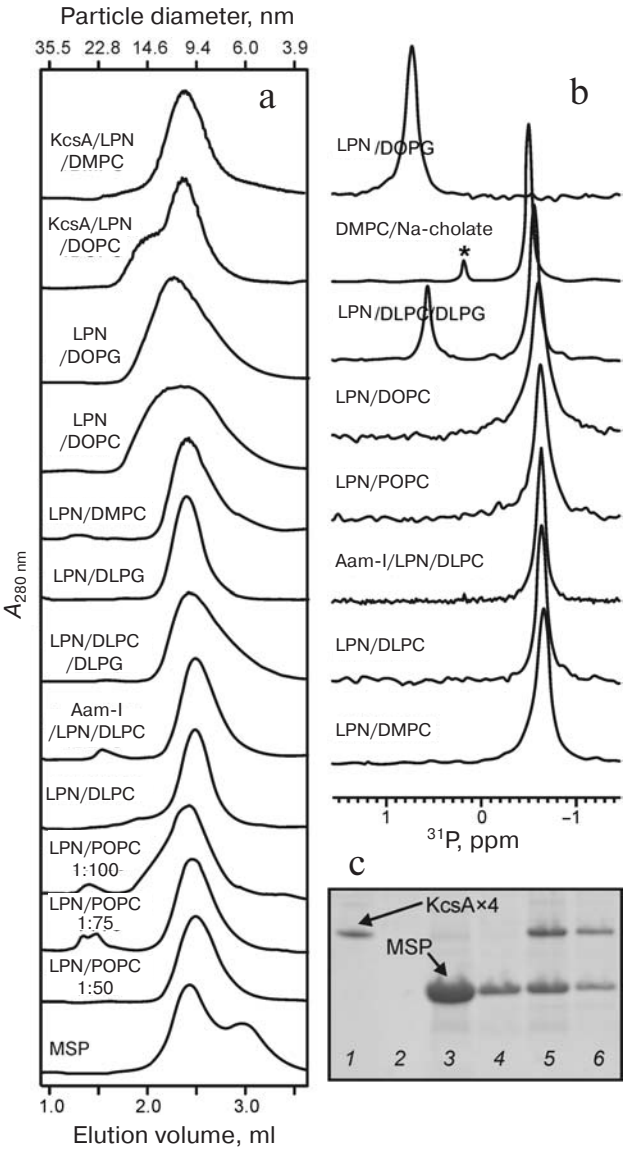

Fig. 1. Biochemical and spectral analyses of LPN preparations. a) Size-exclusion chromatography profiles of free MSP aggregates, "empty" LPNs, and KcsA/LPN and Aam-I/LPN complexes. The particle diameter scale (nm) was obtained using a calibration curve (see "Materials and Methods"). b) ^{31}P-NMR spectra of LPN phospholipid membrane and DMPC solubilized in sodium cholate (25°C). The signal of LMPC impurity in the DMPC/Na-cholate sample is denoted by asterisk. c) Electrophoretic analysis of KcsA/LPN/DMPC complex purification on the metal affinity resin. Lanes: *1*) KcsA tetramer in DDM; *2*) washing with buffer A; *3*, *4*) elution with buffer A containing 100 mM imidazole; *5*, *6*) elution with buffer A containing 500 mM imidazole.

dine sequence from the MSP molecule) into MPs is necessary in most cases for separation of "empty" LPNs and LPNs containing MP [16-19].

Preparation of "empty" LPNs. Dependence of nanodisc diameter on lipid composition. As noted above, both the spectral line width and sensitivity of NMR measurements strongly depend on rotational diffusion rate of a protein molecule in solution and, hence, on its size. One could expect that the effective rotational diffusion rate of MP embedded in LPN should primarily depend on the nanodisc diameter. Thus, the smallest LPNs that still retain their membrane-mimicking properties are optimal for NMR spectroscopy. Numerous studies clearly show that both full-size apoA-1 and its fragment 44-243 (MSP) can form a discrete-sized series of lipoprotein particles [12, 22]. To prepare stable LPNs of smallest size, we optimized lipid (POPC) amounts added to the reaction mixture for reconstruction of nanodiscs. We tested the following MSP/POPC molar ratios: 1 : 50, 1 : 75, and 1 : 100. The LPNs prepared were purified on the Ni^{2+}-affinity resin and analyzed by size-exclusion chromatography (the table and Fig. 1a). As one can see on the figure, the LPN diameter is 9.5 ± 0.5 nm at 1 : 50 or 1 : 75 MSP/lipid ratio. With the increase in lipid concentration to 1 : 100, the formation of larger diameter particles (~12 nm) leads to noticeable decrease in sample homogeneity (Fig. 1a). On the other hand, the final yield of the nanodisc reconstruction determined from the concentration of MSP embedded in LPNs was twofold higher at 1 : 75 ratio than that at 1 : 50 ratio; in the latter case the excess of MSP exists in the form of aggregates. Thus, the MSP/lipid ratio of 1 : 75 is the optimum for the formation of POPC-based "empty" nanodiscs of ~9.5 nm diameter.

Our data are in good agreement with a modern concept of LPN structure (Scheme). Let us suppose that the nanodisc is composed of two MSP molecules and lipid bilayer of 150 POPC molecules, then the area of the bilayer fragment (~49 nm^2) corresponds to diameter ~8 nm; given double thickness of the MSP molecule in helical conformation, the overall LPN diameter is about 10 nm, which is consistent with the results of size-exclusion chromatography. Taking into account the similar surface area values (0.6-0.7 nm^2/molecule) for all lipids used in our work, we used the MSP/lipid ratio of 1 : 75 in all further experiments on "empty" LPN reconstruction. The data of size-exclusion chromatography of "empty" LPNs containing DLPC, DLPG, DMPC, DOPC, DOPG, as well as DLPC/DLPG (4 : 1) mixture are shown on the Fig. 1a and in the table. The table shows that the diameter of LPNs formed by zwitterionic saturated lipids (DLPC, DMPC) is about 10 nm, which is close to the expected value. However, the use of zwitterionic lipid with two unsaturated fatty acid chains (DOPC) led to an increase in nanodisc diameter. We observed the same effect (LPN diameter increase) when used charged lipids: addition of even 20% charged lipid (DLPG) led to noticeable increase in nanodisc diameter (Fig. 1a and the table). This effect is probably associated with decrease in packing density of nanodisc membrane caused either by negative charge repulsion or the presence of double bonds in both chains of the lipid molecule. The greatest LPN size (11.6 nm) was achieved when DOPG (table) combining both features was used.

Dependence of size of LPNs and MSP complexes on lipid composition and MSP/lipid molar ratio

Complex composition	MSP/lipid molar ratio	Diameter of complex, nm (±0.5 nm)
MSP	–	6.0, 10.1
LPN/POPC	1 : 50	9.4
–"–	1 : 75	9.5
–"–	1 : 100	10.1
LPN/DLPC	1 : 75	9.5
Aam-1/LPN/DLPC	1 : 75	9.6
LPN/DLPC/DLPG	1 : 75	9.8
LPN/DLPG	1 : 75	10.5
LPN/DMPC	1 : 75	10.0
LPN/DOPC	1 : 75	10.9
LPN/DOPG	1 : 75	11.6
KcsA/LPN/DMPC	1 : 40	10.9
KcsA/LPN/DOPC	1 : 40	10.9, 16.6

All prepared samples of "empty" LPNs except DLPG-based nanodiscs were stable for no less than three months at room temperature and no less than one week at 45°C. LPNs formed by DLPG were unstable and disintegrated in several days forming lipid precipitate. This effect is probably associated with relatively high solubility of DLPG due to both short fatty acid chains and charged polar head of the lipid.

^{31}P-NMR spectroscopy of nanodisc phospholipid membranes. We used ^{31}P-NMR spectroscopy for testing a theoretical prediction on isotropic reorientation of LPN in solution (Fig. 1b). The spectrum of nanodisc phospholipid membranes composed of phosphatidylcholine revealed single narrow isotropic signal in the region from –0.6 to –0.7 ppm, whereas membranes composed of phosphatidylglycerol had a signal in the region from 0.7 to 0.8 ppm. These data are consistent with the values of isotropic chemical shifts of the lipids in the liposomes observed by magic-angle spinning (MAS) solid-state NMR spectroscopy [31]. This suggests isotropic rotation of LPN in solution and absence of preferential orientation of the LPN particles in the magnetic field of the NMR spectrometer. It is worth noting that LPN composed of DLPC/DLPG (4 : 1) mixture exhibits a shift of signals of phosphatidylcholine and phosphatidylglycerol phosphate moieties in direction to values observed for the lipids solubilized with sodium cholate (–0.5 and 0.5 ppm, respectively [28]) (Fig. 1b).

Reconstruction of lipid–protein nanodiscs containing KcsA. The feasibility of NMR spectroscopy for studies of membrane proteins integrated in LPN membranes was tested using ^{15}N-labeled potassium channel KcsA from *Streptomyces lividans*. According to data of X-ray structural analysis and NMR spectroscopy [32-34], KcsA is composed of four equal subunits surrounding the channel pore (Scheme). Each subunit, in turn, includes N- and C-terminal helical domains exposed to solvent and a TM-domain composed of two TM-helices, additional P-helix, and a selective filter.

The recombinant KcsA tetramer isolated from bacterial membrane of *Escherichia coli* and solubilized in DDM was used for reconstruction of KcsA/LPN. We tested different lipid compositions for LPN formation: zwitterionic lipids (DOPC, DMPC, and POPC) and partially anionic mixture DOPG/DOPE (7 : 3). The prepared nanodiscs were examined by SDS-PAGE (Fig. 1c) and size-exclusion chromatography (Fig. 1a and the table). We observed formation of complexes containing the KcsA tetramer in all cases, but not in the DOPG/DOPE mixture. Gel filtration of the complexes showed that nanodiscs composed of POPC and DMPC are the most homogeneous (particle diameter ~10.1 nm). The DOPC-based LPN sample (Fig. 1a) contained an admixture of larger particles (diameter > 16 nm), which was probably due to embedding of several copies of the tetrameric KcsA in one nanodisc. When DOPG/DOPE-based nanodiscs were formed, the KcsA tetramers dissociated into monomers, and MP precipitation was observed. This contradicts published data indicating that the DOPG/DOPE mixture is optimal for KcsA renaturation *in vitro* [35]. Inefficiency of nanodisc formation with this composition is probably associated with the inability of the MSP molecule to stabilize the lipid bilayer with the strong negative spontaneous curvature due to phosphatidylethanolamine molecules.

Given a supposition that denser packing of saturated lipids might reduce the intramolecular MP dynamics, which worsens the quality of NMR spectra, we decided to use DMPC for the reconstruction of LPNs containing the ^{15}N-labeled KcsA. All stages of reconstruction, purification, and dialysis were performed at a temperature above the DMPC phase transition temperature (24°C). Different KcsA/MSP ratios (1 : 10 and 1 : 20) and MSP/DMPC ratios (1 : 20, 1 : 40, 1 : 75, and 1 : 100) were checked for optimization of reconstruction. The most effective incorporation (~70%) was observed at the ratios KcsA/MSP 1 : 20 and MSP/DMPC 1 : 40. These ratios were further used for the preparation of sample containing the ^{15}N-labeled KcsA.

NMR spectroscopy of ^{15}N-KcsA embedded in nanodiscs. The 40-50 intense signals with $^{1}H_N$ $\Delta\nu$ ~20-30 Hz were observed in the 2D ^{1}H-^{15}N-HSQC spectrum of the KcsA/LPN/DMPC complex (data not shown). Comparison of this spectrum with those of ^{2}H-^{15}N-labeled KcsA in micelles of DPC and SDS [33, 34] shows that the observed signals belong to the N- and C-terminal helical domains of the channel exposed to solvent. The use of the TROSY method led to insignificant narrowing

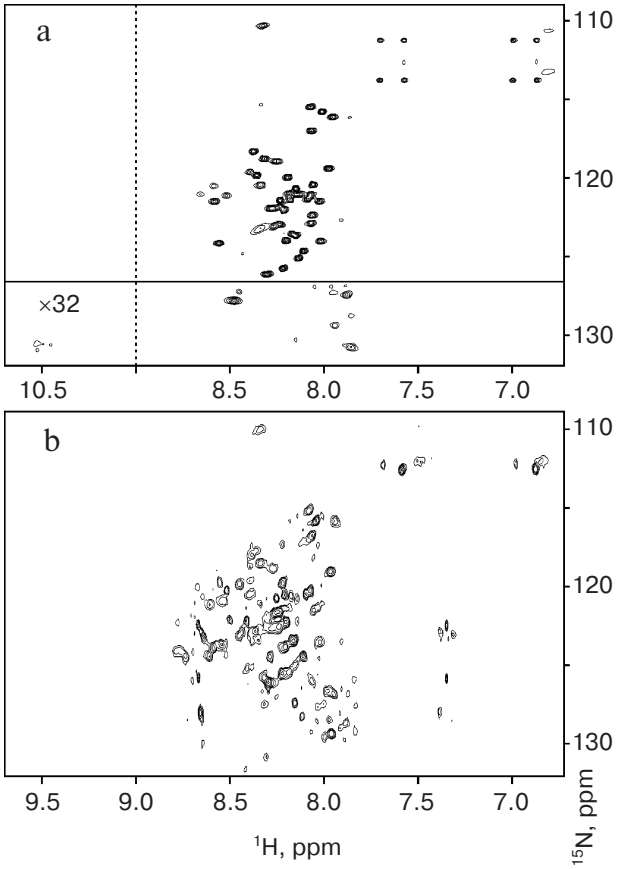

Fig. 2. 2D ^{1}H-^{15}N-TROSY spectra of KcsA/LPN/DMPC complexes (0.1 mM KcsA tetramer, 45°C, pH 3.8). a) H_2O solution (5% D_2O), intensity of spectral fragment on the inset are 32-fold increased. b) D_2O solution (less than 5% H_2O). The exchange of amide protons of KcsA by deuterium was carried out during 60 days at room temperature.

of these signals (on an average 3-5 Hz), but broader and weaker signals (^1H_N $\Delta\nu$ ~50-80 Hz) appeared, which seem to belong to the transmembrane domain of the channel (Fig. 2a). Identification of these "broad" signals is severely hampered on the background of "narrow" signals. Using repeated cycles of dilution–concentration, the D_2O level in the KcsA/LPN/DMPC sample was elevated from 5 to 95% to weaken the intensity of NMR-signals from the KcsA domains exposed to the solvent. According to data from the literature [33], we expected that in 95% D_2O solution all HN-protons of the exposed domains would be replaced by deuterium of the solvent after two months at room temperature, whereas the HN-protons of the TM domains, which are shielded from the solvent by the LPN membrane, would undergo virtually no exchange. The 2D ^{1}H-^{15}N-TROSY spectrum recorded 60 days later confirmed our expectation: the intensity of "narrow" signals significantly decreased to expose a large number of "broad" signals (Fig. 2b). The ^{31}P-NMR analysis of KcsA/LPN/DMPC complexes confirmed the isotropic rotational character of these particles in solution (data not shown). The prepared KcsA/LPN sample was stable for 8 months.

Incorporation of Aam-I in lipid–protein nanodiscs. The feasibility of high-resolution NMR spectroscopy for studies of membrane-active peptides integrated in LPN membrane was tested using ^{15}N-labeled of Aam-I (Ac-Phe^1-Aib-Aib-Aib-Iva-Gly-Leu-Aib^8-Aib-Hyp-Gln-Iva-Hyp-Aib-Pro-Phl^{16}, where Aib is α-aminoisobutyric acid, Iva is isovaline, Hyp is hydroxyproline, and Phl is phenylalaninol). This antibiotic isolated from a fungus of the family Emericellopsis is poorly soluble in water (the upper limit of solubility is 30 μM), forms bent right-handed helix in surrounding of anisotropic membrane-mimicking media (DMPC/DHPC bicelles, various micelles), and demonstrates quick exchange between several conformations with different helix handedness in the isotropic membrane mimetic methanol [26].

A modified protocol we developed earlier [23] was used for preparation of Aam-I/LPN complexes. ^{15}N-Labeled Aam-I dissolved in methanol was added portion-wise to samples of "empty" nanodiscs containing DLPC, DMPC, POPC, or DOPG. Incubation of the mixtures in Eppendorf tubes with open lids for 1 h at 30°C with agitation resulted in partial evaporation of methanol and embedding of the peptide in the LPN membrane. The final concentration of deuterated methanol (C^2H_3OH) in samples was determined by ^{2}H-NMR and did not exceed 2%. This method allows both achievement of comparatively high peptide concentration (~0.5 mM) and prevention of LPN destruction that might be caused by high methanol concentrations. The Aam-I/LPN complexes were examined by size-exclusion chromatography and ^{31}P-NMR spectroscopy (Fig. 1, a and b). According to the data, embedding of the peptide in the nanodisc membrane (at peptide/lipid ratio 1 : 30) did not lead to significant changes in LPN size and lipid packing of LPN membrane.

Comparison of sensitivity of different methods for NMR spectroscopy of polypeptide molecules embedded in nanodiscs. Using the prepared Aam-I/LPN samples, we compared different experimental schemes (HSQC, HMQC, TROSY) for measurement of 2D ^{1}H-^{15}N-correlation spectra of polypeptides embedded in the nanodisc membrane. The most sensitive method was HMQC [5] with magnetization transfer time reduced to 3 msec, including elements of gradient echo for choice of magnetization transfer pathways, as well as binomial sequence and amplitude-modulated pulses to prevent water signal saturation. Both HSQC and TROSY methods including special elements for sensitivity enhancement and amplitude-modulated pulses at the water signal frequency [36, 37] were on average 35% less sensitive. However, the TROSY scheme allows effective narrowing of spectral lines, for instance, ^1H_N $\Delta\nu$ reduction was 10-15 Hz (Fig. 3, a and d).

High sensitivity of the HMQC scheme is explained by summation of magnetization transferred in two ways:

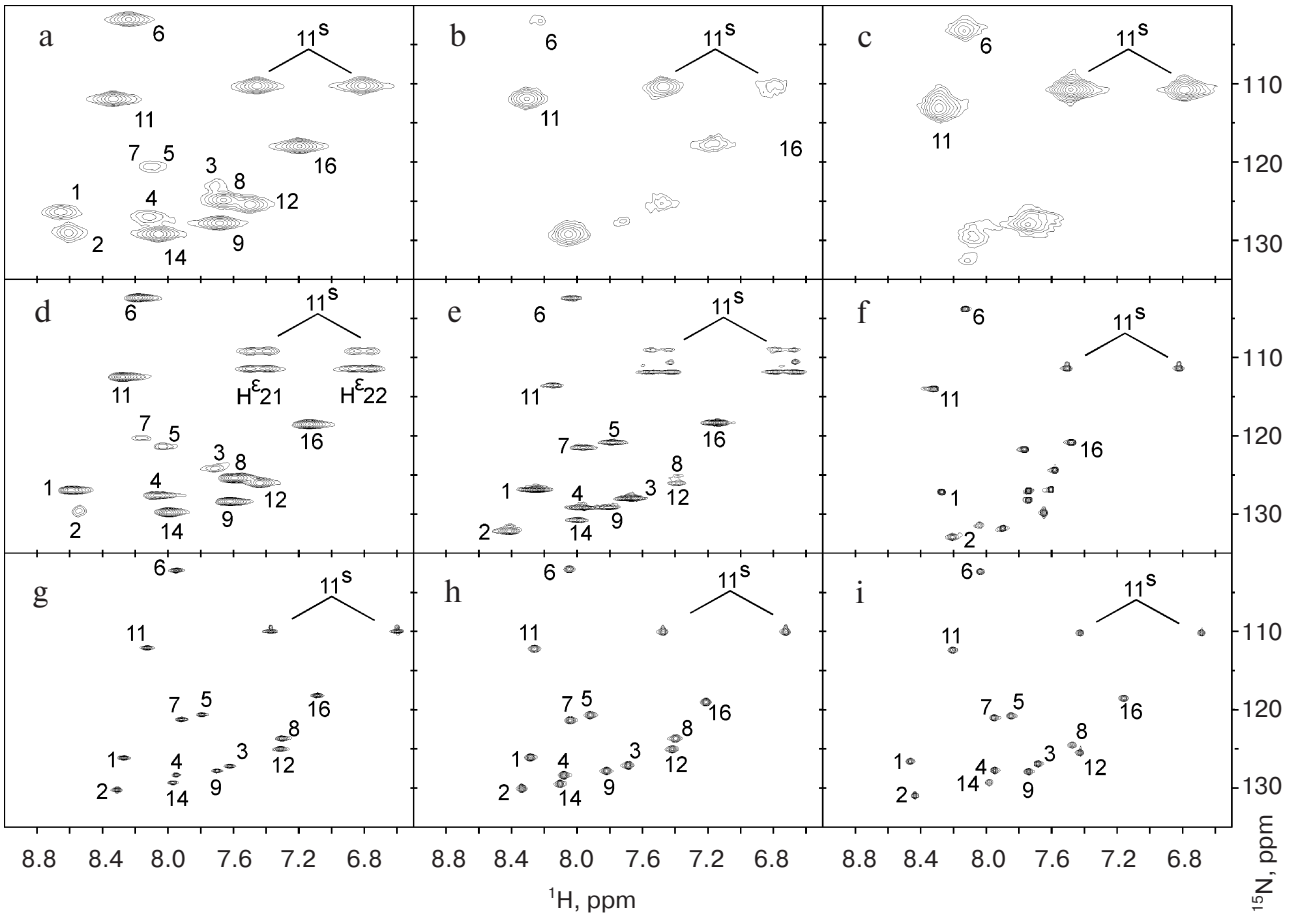

Fig. 3. 2D ^{1}H-^{15}N correlation spectra of Aam-I in LPN/DLPC (a, d), LPN/DMPC (b), LPN/POPC (c), LPN/DOPG (e), 2% methanol (f), LMPC micelles (g), LMPG micelles (h), or DMPC/DHPC (1 : 4) bicelles (i). Known schemes [36, 37] were used for recording TROSY (d, e) and HSQC (f-i) spectra; the scheme with magnetization transfer time reduced to 3 msec [5] including additional elements (see "Results") was used for recording HMQC spectra (a-c). The spectra of Aam-I in LPN were recorded at 45°C and spectra of Aam-I in 2% methanol, micelles, or bicelles at 40°C.

via J-coupling constants and cross-correlated relaxation (CRINEPT-type scheme) [5]. In this context, phase cycles of HSQC and TROSY experiments effectively suppress the latter way (INEPT-type scheme). It is worth noting that, unlike CRINEPT schemes, which were earlier applied for NMR-spectroscopy of large (up to 1000 kDa) protein complexes with deuterated side chains [5, 7], we used the HMQC variant with decoupling from ^{15}N at the moment of detection. The absence of expected gain in sensitivity of TROSY compared with HSQC in the case of Aam-I/LPN complexes seems to be also due to the absence of peptide side-chain deuteration.

NMR spectroscopy of ^{15}N-Aam-I embedded in nanodiscs. The 2D ^{1}H-^{15}N NMR-spectra of Aam-I embedded in LPN membranes of different composition are shown in Fig. 3 (a-e). The spectra of Aam-I in 2% methanol and in a number of commonly used membrane-mimicking media are given on this figure for comparison. A shift in the position of signals from the peptide and their substantial broadening, as compared with the peptide spectrum in 2% methanol, suggests the embedding of Aam-I into LPN membranes. At the same time, the observed width of Aam-I signals ($^{1}H_N$ $\Delta\nu$ 50-60 Hz, in TROSY spectra at 45°C) and the measured rate of the cross-correlation process between the dipole–dipole and chemical shift anisotropy relaxation of ^{15}N nuclei (η_{XY} ~ 52 Hz at 800 MHz at 45°C) corresponded to the effective rotational correlation time τ_R ~ 40 nsec. The resulting value was lower than expected for discoid particle of 10 × 4 nm in size (56-61 nsec, see above). That points to the presence of additional degrees of freedom for Aam-I in the complex with the nanodisc. (The value τ_R ~ 40 nsec corresponds to isotropic reorientation of a protein particle with molecular mass of ~100 kDa and R_{St} ~ 4.1 nm.)

The most interesting property of LPN-embedded antiamoebin spectra was the selective exchange broadening (and, correspondingly, disappearance from the spectrum) observed for a number of signals. So, only 2-3 intense signals from the main chain of the peptide were observed in DMPC and POPC membranes (Fig. 3, b and

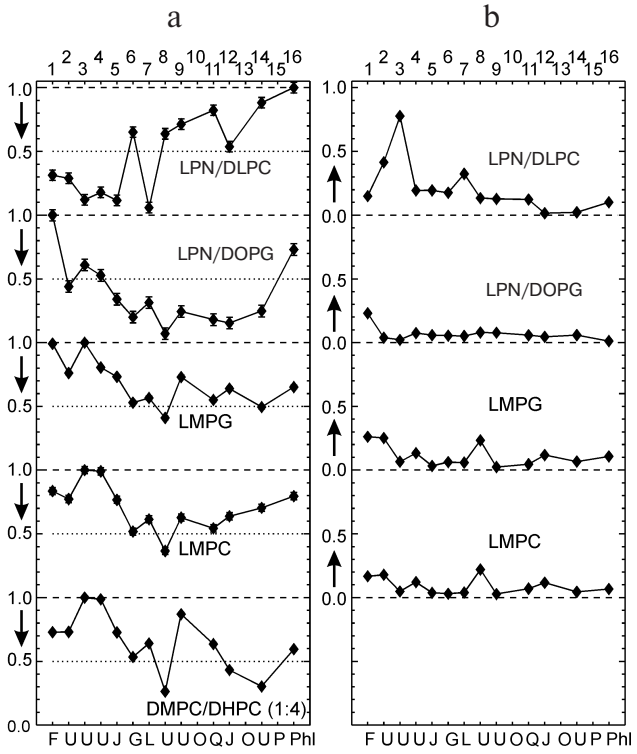

Fig. 4. Comparison of spectral characteristics of Aam-I embedded in LPN/DLPC, LPN/DOPG, LMPC micelles, LMPG micelles, and DMPC/DHPC (1 : 4) bicelles. a) Normalized amplitude (intensity) of backbone ^{1}H-^{15}N cross-peaks. b) Change in reduced chemical shift of backbone $^{1}H^{15}N$-groups of the main peptide chain $\left(\sqrt{\left(\Delta\delta^{1}H\right)^{2}+\left(\Delta\delta^{15}N/5\right)^{2}}\right)$ in various media in comparison with DMPC/DHPC (1 : 4) bicelles.

c); moreover, two protons from the NH_2-group of the Gln11 side chain demonstrated different signal intensities in LPN/DMPC (Fig. 3b). A selective broadening of signals from the N-terminal part of the peptide was observed in DLPC membranes (Fig. 3, a and d). In DOPG membranes, the signal from the Aib8 NH-group located in the central part of the peptide was substantially broadened (Fig. 3e). The selective broadening of signals suggests exchange between several membrane-bound peptide states (so-called "conformational exchange" [38]). The observed processes apparently differ in membranes of different composition, and the minimum broadening of signals was observed in the DOPG membrane, which demonstrates the lowest density of lipid packing (see above).

Chemical shifts and amplitudes of signals from HN-groups of the peptide were used for comparison of the structure and dynamics of Aam-I embedded in nanodisc membranes (DLPC, DOPG) with those of Aam-I embedded in classical membrane mimetics (DMPC/DHPC bicelles, LMPC and LMPG micelles) (Fig. 4, a and b). We supposed that the alterations in the spatial structure of the peptide would result in changes in chemical shifts, and the appearance of exchange processes would induce broadening of the signals and, correspondingly, decrease in their intensities. These results suggest similarity between the structure and dynamic mobility of LPN/DOPG-embedded Aam-I with those observed in classical membrane mimetics. So, for instance, only one signal (HN Phe1) demonstrates a substantial shift compared with DMPC/DHPC bicelles, and the broadening of the signal from the HN-group of Aib8 is observed in both DMPC/DHPC bicelles and LMPC and LMPG micelles. However, the structure and dynamic mobility of the DLPC-embedded peptide differ substantially. This seems to result from different topology of Aam-I embedded in LPN membranes formed from short (DLPC, fatty acid chain length is 12 C-atoms and hydrophobic thickness is 2.4 nm) and long (DOPG, fatty acid chain length is 18 C-atoms and hydrophobic thickness is 2.7 nm) lipids. Aam-I having the length of ~2.7 nm interacts at its periphery with DOPG membrane surface (similar to micelles and bicelles [23]), but perhaps occupies a transmembrane position in DLPC membranes.

DISCUSSION

The results of the present work demonstrate the possibility of using lipid–protein nanodiscs for NMR studies of both membrane proteins and membrane-active peptides. Nanodiscs possess a number of unique properties, as compared with classic mimetics, micelles, and small spherical bicelles routinely used in NMR spectroscopy. Nanodiscs are more stable, and the fragment of flat bilayer membrane in the nanodisc represents a substantially better model of biological membrane than the spherical dynamically mobile surface of a bicelle or micelle. Unlike lipid vesicles, LPNs are smaller in size, which substantially increases the number of experimental techniques that can be used for the study of embedded proteins. The LPNs allow a change of the sample buffer by dialysis and can be easily diluted or concentrated. Besides, integral proteins embedded into nanodiscs are protected from unfavorable intermolecular interactions [18], which stabilizes the protein sample for a long time. The usage of various lipids and their mixtures for nanodisc formation offers new possibilities for studies of membrane proteins in their natural environment.

The main drawback of the proposed medium is the relatively large sizes of membrane-mimicking complexes resulting in substantial increase in the rate of transverse relaxation of nuclear magnetization, increase in width of signals, and, correspondingly, decrease in sensitivity of NMR experiments. In the present work we have recorded interpretable NMR spectra of the mobile domains of the KcsA potassium channel exposed to a solution and spectra of Aam-I peptide associated with the membrane sur-

face of a nanodisc, but possibly undergoing rapid rotation around the axis perpendicular to the LPN membrane. In the latter case, the width of the NMR signals (^1H_N $\Delta\nu$) comprised 50-60 Hz. For TM domains of integral membrane proteins embedded into nanodisc membranes, one can anticipate still broader signals. One possible solution to this problem is partial or total deuteration of side chains of the studied protein molecule [3]. The recent progress in the development of new schemes of isotopic labeling and new NMR spectroscopy methods [3-7] opens new avenues for successful application of nanodiscs for NMR studies of membrane proteins and peptides.

The authors are indebted to staff members of the Center of Instrumental Methods and Innovation Technologies for Analysis of Substances at the Russian University of People's Friendship for the kindly provided access to the JEOL ECA-600 NMR spectrometer and for their assistance in recording ^{31}P-NMR spectra.

This study was supported by the Russian Federation President's Grants (MK-6346.2008.4 and SS-1061.2008.4), by MCB program of Russian Academy of Sciences, and by the Russian Foundation for Basic Research grants (06-04-49413 and 08-04-01442).

REFERENCES

1. Wuthrich, K. (1986) *NMR of Proteins and Nucleic Acids*, John Wiley and Sons, New York.
2. Cavanagh, J., Fairbrother, W. J., Palmer III, A. G., Skelton, N. J., and Rance, M. (2006) *Protein NMR Spectroscopy: Principles and Practice*, 2nd Edn., Academic Press.
3. Tugarinov, V., Kanelis, V., and Kay, L. E. (2006) *Nat. Protoc.*, **1**, 749-754.
4. Pervushin, K., Riek, R., Wider, G., and Wuthrich, K. (1997) *Proc. Natl. Acad. Sci. USA*, **94**, 12366-12371.
5. Riek, R., Fiaux, J., Bertlesen, E. B., Horwich, A. L., and Wuthrich, K. (2002) *J. Am. Chem. Soc.*, **124**, 12144-12153.
6. Tugarinov, V., Choy, W. Y., Orekhov, V. Y., and Kay, L. E. (2005) *Proc. Natl. Acad. Sci. USA*, **102**, 622-627.
7. Horst, R., Bertelsen, E. B., Fiaux, J., Wider, G., Horwich, A. L., and Wuthrich, K. (2005) *Proc. Natl. Acad. Sci. USA*, **102**, 12748-12753.
8. Sanders, C. R., and Sonnichsen, F. (2006) *Magn. Reson. Chem.*, **44**, S24-S40.
9. Page, R. C., Moore, J. D., Nguyen, H. B., Sharma, M., Chase, R., Gao, F. P., Mobley, C. K., Sanders, C. R., Ma, L., Sonnichsen, F. D., Lee, S., Howell, S. C., Opella, S. J., and Cross, T. A. (2006) *J. Struct. Funct. Genom.*, **7**, 51-64.
10. Krueger-Koplin, R. D., Sorgen, P. L., Krueger-Koplin, S. T., Rivera-Torres, I. O., Cahill, S. M., Hicks, D. B., Grinius, L., Krulwich, T. A., and Girvin, M. E. (2004) *J. Biomol. NMR*, **28**, 43-57.
11. Chou, J. J., Kaufman, J. D., Stahl, S. J., Wingfield, P. T., and Bax, A. (2002) *J. Am. Chem. Soc.*, **124**, 2450-2451.
12. Li, L., Chen, J., Mishra, V. K., Kurtz, J. A., Cao, D., Klon, A. E., Harvey, S. C., Anantharamaiah, G. M., and Segrest, J. P. (2004) *J. Mol. Biol.*, **343**, 1293-1311.
13. Shih, A. Y., Denisov, I. G., Phillips, J. C., Sligar, S. G., and Schulten, K. (2005) *Biophys. J.*, **88**, 548-556.
14. Wu, Z., Wagner, M. A., Zheng, L., Parks, J. S., Shy, J. M., Smith, J. D., Gogonea, V., and Hazen, S. L. (2007) *Nat. Struct. Mol. Biol.*, **14**, 861-868.
15. Matz, C. E., and Jonas, A. (1982) *J. Biol. Chem.*, **257**, 4535-4540.
16. Nath, A., Atkins, W. M., and Sligar, S. G. (2007) *Biochemistry*, **46**, 2059-2069.
17. Bayburt, T. H., and Sligar, S. G. (2003) *Prot. Sci.*, **12**, 2476-2481.
18. Whorton, M. R., Bokoch, M. P., Rasmussen, S. G. F., Huang, B., Zare, R. N., Kobilka, B., and Sunahara, R. K. (2007) *Proc. Natl. Acad. Sci. USA*, **104**, 7682-7687.
19. Banerjee, S., Huber, T., and Sakmar, T. P. (2008) *J. Mol. Biol.*, **377**, 1067-1081.
20. Denisov, I. G., McLean, M. A., Shaw, A. W., Grinkova, Y. V., and Sligar, S. G. (2005) *J. Phys. Chem. B.*, **109**, 15580-15588.
21. Bayburt, T. H., Grinkova, Y. L., and Sligar, S. G. (2002) *Nano Lett.*, **2**, 853-856.
22. Denisov, I. G., Grinkova, Y. V., Lazarides, A. A., and Sligar, S. G. (2004) *J. Am. Chem. Soc.*, **126**, 3477-3487.
23. Lyukmanova, E. N., Shenkarev, Z. O., Paramonov, A. S., Sobol, A. G., Ovchinnikova, T. V., Chupin, V. V., Kirpichnikov, M. P., Blommers, M. J., and Arseniev, A. S. (2008) *J. Am. Chem. Soc.*, **130**, 2140-2141.
24. Nekrasova, O. V., Ignatova, A. A., Nazarova, A. I., Feofanov, A. V., Korolkova, Y. V., Boldyreva, E. F., Tagvei, A. I., Grishin, E. V., Arseniev, A. S., and Kirpichnikov, M. P. (2009) *J. Neuroimmune Pharmacol.*, **4**, 83-91.
25. Heginbotham, L., Odessey, E., and Miller, C. (1997) *Biochemistry*, **36**, 10335-10340.
26. Shenkarev, Z. O., Paramonov, A. S., Nadezhdin, K. D., Bocharov, E. V., Kudelina, I. A., Skladnev, D. A., Tagaev, A. A., Yakimenko, Z. A., Ovchinnikova, T. V., and Arseniev, A. S. (2007) *Chem. Biodivers.*, **4**, 1219-1242.
27. Wishart, D. S., Bigam, C. G., Yao, J., Abildgaard, F., Dyson, H. J., Oldfield, E., Markley, J. L., and Sykes, B. D. (1995) *J. Biomol. NMR*, **6**, 135-140.
28. Pearce, J. M., and Komoroski, R. A. (1993) *Magn. Reson. Med.*, **29**, 724-731.
29. Lee, D., Hilty, C., Wider, G., and Wuthrich, K. (2006) *J. Magn. Reson.*, **178**, 72-76.
30. Ortega, A., and de la Torre, J. G. (2003) *J. Chem. Phys.*, **119**, 9914-9919.
31. Carbone, M. A., and Macdonald, P. M. (1996) *Biochemistry*, **35**, 3368-3378.
32. Doyle, D. A., Morais, C. J., Pfuetzner, R. A., Kuo, A., Gulbis, J. M., Cohen, S. L., Chait, B. T., and MacKinnon, R. (1998) *Science*, **280**, 69-77.
33. Chill, J. H., Louis, J. M., Miller, C., and Bax, A. (2006) *Prot. Sci.*, **15**, 684-698.
34. Baker, K. A., Tzitzilonis, C., Kwiatkowski, W., Choe, S., and Riek, R. (2007) *Nat. Struct. Mol. Biol.*, **14**, 1089-1095.
35. Chupin, V. V., Nekrasova, O. V., Kirpichnikov, M. P., and Arseniev, A. S. (2007) Patent of RF No. 2306319, September 20, 2007.
36. Schleucher, J., Schwendinger, M., Sattler, M., Schmidt, P., Schedletzky, O., Glaser, S. J., Sorensen, O. W., and Griesinger, C. (1994) *J. Biomol. NMR*, **4**, 301-306.
37. Nietlispach, D. (2005) *J. Biomol. NMR*, **31**, 161-166.
38. Palmer III, A. G., Kroenke, C. D., and Loria, J. P. (2001) *Meth. Enzymol.*, **339**, 204-238.